

Bilayer graphene: gap tunability and edge properties

Eduardo V Castro¹, N M R Peres², J M B Lopes dos Santos¹,
F Guinea³ and A H Castro Neto⁴

¹ CFP and Departamento de Física, Faculdade de Ciências Universidade do Porto, P-4169-007 Porto, Portugal

² Center of Physics and Departamento de Física, Universidade do Minho, P-4710-057 Braga, Portugal

³ Instituto de Ciencia de Materiales de Madrid, CSIC, Cantoblanco, E-28049 Madrid, Spain

⁴ Department of Physics, Boston University, 590 Commonwealth Avenue, Boston, MA 02215, USA

E-mail: evcastro@fc.up.pt

Abstract. Bilayer graphene – two coupled single graphene layers stacked as in graphite – provides the only known semiconductor with a gap that can be tuned externally through electric field effect. Here we use a tight binding approach to study how the gap changes with the applied electric field. Within a parallel plate capacitor model and taking into account screening of the external field, we describe real back gated and/or chemically doped bilayer devices. We show that a gap between zero and midinfrared energies can be induced and externally tuned in these devices, making bilayer graphene very appealing from the point of view of applications. However, applications to nanotechnology require careful treatment of the effect of sample boundaries. This being particularly true in graphene, where the presence of edge states at zero energy – the Fermi level of the undoped system – has been extensively reported. Here we show that also bilayer graphene supports surface states localized at zigzag edges. The presence of two layers, however, allows for a new type of edge state which shows an enhanced penetration into the bulk and gives rise to band crossing phenomenon inside the gap of the biased bilayer system.

1. Introduction

The recent production of graphene [1], the first truly one-atom thick material, enabled several unthoughtful experiments where charge carriers were undoubtedly shown to be massless with a linear dispersion relation [2].

In addition to single layer graphene (SLG), few-layer graphene can also be isolated. Of particular interest to us is the double layer graphene system, where two carbon layers are placed on top of each other according to the usual Bernal *AB*-stacking. The low-energy properties of this so-called bilayer graphene (BLG) are then described by massive Dirac fermions [2], with a quadratic dispersion close to the neutrality point and a Dirac fermion mass originating from the inter-plane hopping energy t_{\perp} .

One of the most remarkable properties of BLG is the ability to open a gap in the spectrum by electric field effect – biased BLG. This has been realized experimentally, providing the first semiconductor whose gap can be tuned externally [3, 4, 5]. In the absence of external perpendicular electric field – unbiased BLG – the system is characterized by four bands, two of them touching each other at zero energy, and giving rise to the massive Dirac fermions mentioned above, and other two separated by an energy $\pm t_{\perp}$. Hence, an unbiased BLG is

a two-dimensional zero-gap semiconductor. At the neutrality point the conductivity shows a minimum of the order of the conductance quantum [6], a property shared with SLG [2]. This prevents standard logic applications where the presence of a finite gap producing high on-off current ratios is of paramount importance. The fact that a simple perpendicular electric field is enough to open a gap, and even more remarkable, to control its value, clearly demonstrates the potential of this system for carbon-based electronics. A new plateau at zero Hall conductivity [5] and ferromagnetic behavior at low densities are some of the gap consequences [7]. Moreover, the induced gap has been shown to be robust to the presence of disorder [8, 9].

Although such a tunable gap by the electric field effect is not possible in SLG, band gaps can still be engineered by confining graphene electrons in narrow ribbons [10, 11]. However, the lateral confinement brings about the presence of edges, which in graphene can have profound consequences on electronics. This is essentially due to the rather different behavior of the two possible (perfect) terminations in graphene: *zigzag* and *armchair*. While zigzag edges support localized states, armchair edges do not [12]. These surface (or edge) states occur at zero energy, the same as the Fermi level of undoped graphene, meaning that low energy properties may be substantially altered by their presence. The self-doping phenomenon [13] and the edge magnetization with consequent gap opening [12] are among edge states driven effects. In BLG, the question regarding the presence of edge states is also pertinent. Firstly, zigzag edges are among the possible terminations in BLG, and secondly, the presence of edges is unavoidable in tiny devices.

The paper is organized as follows: in Sec. 2 the lattice structure of BLG and the tight-binding Hamiltonian are presented; bulk electronic properties are discussed in Sec 3; the presence of edge states localized at zigzag edges of BLG is discussed in Sec. 4; Sec. 5 contains our conclusions.

2. Model

The lattice structure of BLG is shown in Fig. 1(a). Here we consider only *AB*-Bernal stacking, where the top layer has its *A* sublattice on top of sublattice *B* of the bottom layer. We use indices 1 and 2 to label the top and bottom layer, respectively. The basis vectors may be written as $\mathbf{a}_1 = a\hat{e}_x$ and $\mathbf{a}_2 = a(\hat{e}_x - \sqrt{3}\hat{e}_y)/2$, where $a = 2.46 \text{ \AA}$.

In the tight-binding approximation, the in-plane hopping energy, $t \approx 3 \text{ eV}$, and the inter-layer hopping energy, $t_\perp/t \sim 0.1 \ll 1$ [2], define the most relevant energy scales (see Fig. 1). The simplest tight-binding Hamiltonian describing non-interacting π -electrons in BLG then reads:

$$H = -t \sum_{\mathbf{r}, \sigma} \sum_{i=1}^2 [a_{i,\sigma}^\dagger(\mathbf{r})b_{i,\sigma}(\mathbf{r}) + a_{i,\sigma}^\dagger(\mathbf{r})b_{i,\sigma}(\mathbf{r} - \mathbf{a}_1) + a_{i,\sigma}^\dagger(\mathbf{r})b_{i,\sigma}(\mathbf{r} - \mathbf{a}_2) + \text{h.c.}] - t_\perp \sum_{\mathbf{r}, \sigma} [a_{1,\sigma}^\dagger(\mathbf{r})b_{2,\sigma}(\mathbf{r}) + \text{h.c.}] + \frac{V}{2} \sum_{\mathbf{r}, \sigma} [n_{A1}(\mathbf{r}) + n_{B1}(\mathbf{r}) - n_{A2}(\mathbf{r}) - n_{B2}(\mathbf{r})], \quad (1)$$

where $a_{i,\sigma}(\mathbf{r})$ [$b_{i,\sigma}(\mathbf{r})$] is the annihilation operator for electrons at position \mathbf{r} in sublattice *Ai* (*Bi*), $i = 1, 2$, and spin σ , and $n_{Ai}(\mathbf{r})$ and $n_{Bi}(\mathbf{r})$ are number operators. We are interested in the properties of BLG in the presence of a perpendicular electric field – the biased BLG. The external perpendicular electric field gives rise to an electrostatic energy difference between the two layers, which we parametrize by V per electron. The effect of this energy difference between layers is accounted for by the last term in Eq. (1).

3. Bulk electronic properties

In the absence of applied perpendicular electric field the system has four bands given by

$$E_{\mathbf{k}}^{\pm\pm} = \pm \sqrt{\epsilon_{\mathbf{k}}^2 + t_\perp^2/4} \pm t_\perp/2, \quad (2)$$

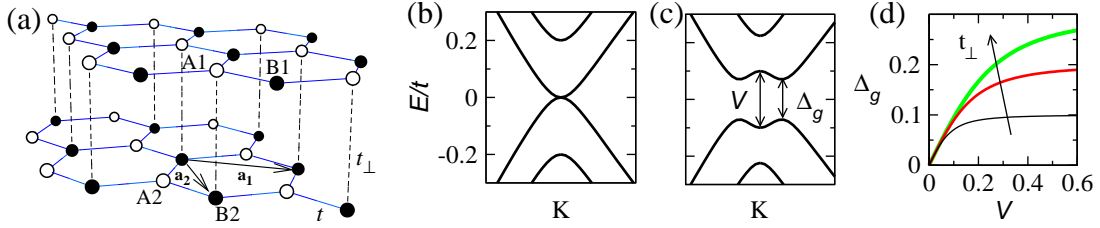


Figure 1. (a) Lattice structure of a graphene bilayer. (b)-(c) Band structure near K (or K') for $V = 0$ and $V = t_{\perp}$, respectively. We used $t_{\perp} = 0.2t$. (d) Variation of the gap Δ_g with V for $t_{\perp} = \{0.1, 0.2, 0.3\}t$.

where $\epsilon_{\mathbf{k}}$ is the dispersion of SLG, $\epsilon_{\mathbf{k}}^2 = t [3 + 2 \cos(ak_x) + 4 \cos(ak_x/2) \cos(ak_y\sqrt{3}/2)]$. The band structure defined by Eq. (2) is shown in Fig. 1(b). In undoped BLG the system has exactly one electron per π orbital, that is, it is a half-filled system. In this case the chemical potential crosses exactly at the K and K' points (the Dirac points) at the corners of the first Brillouin zone. As can be seen in Fig. 1(b), at these corners the dispersion is parabolic, $E(p) \approx \pm v_F^2 p^2 / t_{\perp}$, with $p = \hbar q$, where q measures the distance in momentum space relatively to the Dirac points, and $v_F = \sqrt{3}at\hbar^{-1}/2$ is the SLG Fermi velocity. Thus, low-energy quasiparticles in BLG are massive, with a light effective mass given by $m^* = t_{\perp}/(2v_F^2) \approx 0.03m_e$, where m_e is the bare electron mass [2]. Although this behavior is clearly different from the low-energy massless Dirac fermions found in SLG, $\epsilon(p) \approx \pm v_F p$, it has been shown that the effective 2-band model describing low-energy physics in BLG is still a pseudo-spin Hamiltonian [6]. Consequently, BLG is also far from a standard two-dimensional electron gas; the observed anomalous quantum Hall effect is an example of such an unconventional behavior [6].

Now we address the electronic structure of the biased BLG. The spectrum of Eq. (1) for $V \neq 0$ reads:

$$E_{\mathbf{k}}^{\pm\pm}(V) = \pm \sqrt{\epsilon_{\mathbf{k}}^2 + t_{\perp}^2/2 + V^2/4 \pm \sqrt{t_{\perp}^4/4 + (t_{\perp}^2 + V^2)\epsilon_{\mathbf{k}}^2}}. \quad (3)$$

The resulting band structure is shown in Fig. 1(c). As can be seen from Eq. (3), the $V = 0$ gapless system turns into a semiconductor whose gap is controlled by V . The gap between conduction and valence bands, Δ_g , is given by

$$\Delta_g = \sqrt{t_{\perp}^2 V^2 / (t_{\perp}^2 + V^2)}. \quad (4)$$

Note that V parametrizes the effect of a perpendicular electric field, and therefore can be controlled externally. This means, as a consequence of Eq. (4), that the biased BLG provides a semiconductor with a gap that can be tuned externally by electric field effect. From Eq. (4) it can be seen that for both $V \ll t_{\perp}$ and $V \gg t$ one finds $\Delta_g \sim V$. However, there is a region for $t_{\perp} \lesssim V \lesssim 6t$ where the gap shows a plateau $\Delta_g \sim t_{\perp}$, as depicted in Fig. 1(d). The plateau ends when $V \simeq 6t$ (not shown).

So far we have considered V as a band parameter that controls the gap. However, the parameter V can be related with the perpendicular electric field applied to BLG, avoiding the introduction of an extra free parameter in the present theory. If $\mathbf{E} = E\hat{e}_z$ is the perpendicular electric field felt by electrons in BLG, the corresponding electrostatic energy $U(z)$ for an electron of charge $-e$ is related to the electric field as $eE = \partial U(z)/\partial z$, and thus V is given by

$$V = U(z_1) - U(z_2) = eEd, \quad (5)$$

where z_1 and z_2 is the position of layer 1 and 2, respectively, and $d \equiv z_1 - z_2 = 3.4 \text{ \AA}$ is the inter-layer distance. Given the experimental conditions, the value of E can be calculated under a few assumptions, as detailed in the following.

3.1. Real biased bilayer devices

If we assume the electric field E in Eq. (5) to be due exclusively to the external electric field applied to BLG, $E = E_{ext}$, all we need in order to know V is the value of E_{ext} : $V = eE_{ext}d$. The experimental realization of a biased BLG has been achieved in epitaxial BLG through chemical doping [3] and in back gated exfoliated BLG [5, 4]. In either case the value of E_{ext} can be extracted assuming a simple parallel plate capacitor model.

In the case of exfoliated BLG, devices are prepared by micromechanical cleavage of graphite on top of an oxidized silicon wafer ($t = 300$ nm of SiO_2). A back gate voltage V_g applied between the sample and the Si wafer induces charge carriers due to the electric field effect, resulting in carrier densities $n_g = \alpha V_g$ relatively to half-filling. The geometry of the resulting capacitor determines the coefficient $\alpha = \varepsilon_{\text{SiO}_2} \varepsilon_0 / (et) \cong 7.2 \times 10^{10} \text{ cm}^{-2}/\text{V}$, where $\varepsilon_{\text{SiO}_2} = 3.9$ and ε_0 are the permittivities of SiO_2 and free space, respectively. In order to control independently the gap value and the Fermi level, in Ref. [5] the devices have been chemically doped by deposition of ammonia (NH_3) on top of the upper layer, which adsorbed on graphene and effectively acted as a top gate providing a fixed electron density n_0 . Charge conservation then implies a total density n in BLG given by $n = n_g + n_0$. Extending the parallel plate capacitor model to include the effect of dopants, the external field E_{ext} is the result of charged surfaces placed above and below BLG. The accumulation or depletion layer in the Si wafer contributes with an electric field $E_b = en_g / (2\varepsilon_r \varepsilon_0)$, while dopants above BLG effectively provide the second charged surface with electric field $E_t = -en_0 / (2\varepsilon_r \varepsilon_0)$, where ε_r is the bilayer relative dielectric constant. Adding the two contributions, $E_{ext} = E_b + E_t$, and making use of the charge conservation relation, we arrive at an electrostatic energy difference V that depends linearly on the BLG density,

$$V = (n/n_0 - 2)e^2 n_0 d / (2\varepsilon_r \varepsilon_0). \quad (6)$$

In the case of epitaxial BLG, devices are grown on SiC by thermal decomposition. Due to charge transfer from SiC substrate to film, the as-prepared BLG devices appear electron doped with density n_a . The substrate's depletion layer provides the external electric field necessary to make the system a biased BLG. In Ref. [3] the BLG density n was varied by doping the system with potassium (K) on top of the upper layer, which originates an additional charged layer contributing to the external electric field. Applying the same parallel plate capacitor model as before, we get an electrostatic energy difference that can be written as

$$V = (2 - n/n_a)e^2 n_a d / (2\varepsilon_r \varepsilon_0). \quad (7)$$

In the inset of Fig. 2(a) we compare Eq. (7) with experimental results for V from Ref. [3], obtained by fitting angle resolved photo-emission spectroscopy (ARPES) measurements. For this particular biased BLG realization, the as-prepared carrier density was $n_a \approx 10 \times 10^{12} \text{ cm}^{-2}$. From Eq. (7), this n_a value implies a zero V for the bilayer density $n^{\text{th}} \approx 20 \times 10^{12} \text{ cm}^{-2}$, and therefore zero gap through Eq. (4). Experimentally, a zero gap was found around $n^{\text{exp}} \approx 23 \times 10^{12} \text{ cm}^{-2}$. Given the simplicity of the theory, it can be said that n^{th} and n^{exp} are in good agreement. However, the agreement is only good at $V = 0$, since the measured V is not a linear function of n , as Eq. (7) implies. This is an indication that screening due to correlation effects should be taken into account.

3.2. Screening correction and gap behavior

In deriving Eqs. (6) and (7) we assumed that the electric field E in the BLG region was exactly the external one, E_{ext} . There is, however, an obvious additional contribution: the external electric field polarizes the BLG, inducing some charge asymmetry between the two graphene layers, which in turn give rise to an internal electric field, E_{int} , that screens the external one.

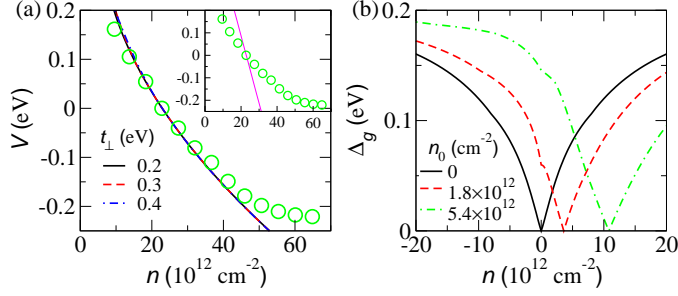


Figure 2. (a) V vs density for the epitaxial biased BLG device. Experimental data from Ref. [3] is shown as \circ . The line in the inset shows the unscreened result given by Eq. (7). (b) Gap vs density for the exfoliated biased BLG device with chemical doping set to n_0 .

To estimate E_{int} we can again apply a parallel plate capacitor model. The internal electric field due to the charge asymmetry between planes may thus be written as $E_{int} = e\Delta n/(2\epsilon_r\epsilon_0)$, where $-e\Delta n$ is the induced charge imbalance between layers, which can be estimated through the weight of the wave functions in each layer,

$$\Delta n = n_1 - n_2 = \frac{2}{N_c A_{\square}} \sum_{j,l=\pm} \sum'_{\mathbf{k}} (|\varphi_{A1,\mathbf{k}}^{jl}|^2 + |\varphi_{B1,\mathbf{k}}^{jl}|^2 - |\varphi_{A2,\mathbf{k}}^{jl}|^2 - |\varphi_{B2,\mathbf{k}}^{jl}|^2), \quad (8)$$

where the factor 2 comes from spin degeneracy, N_c is the number of unit cells and $A_{\square} = a^2\sqrt{3}/2$ is the unit cell area, jl is a band label, and the prime sum runs over all occupied \mathbf{k} 's. Note that in order to calculate Δn we must specify V , as it determines the amplitudes on the right hand side of Eq. (8). On the other hand, Δn determines E_{int} , and in its turn E_{int} enters Eq. (5) through E to give V . Thus, a self-consistent procedure must be followed to calculate the screened energy difference between layers V . In particular, for the two experimental realizations of biased BLG discussed in Sec. 3.1, the self-consistent equation that determines V reads

$$V = [n - 2n_0 + \Delta n(n, V)]e^2 d/(2\epsilon_r\epsilon_0) \quad \text{and} \quad V = [2n_a - n + \Delta n(n, V)]e^2 d/(2\epsilon_r\epsilon_0), \quad (9)$$

respectively for exfoliated BLG [5] and epitaxial BLG [3] devices. It is worth noting that the screening correction expressed in Eq. (9) leads to a term in the Hamiltonian which is exactly the Hartree correction due to the charge asymmetry between layers. This approach has been followed in Refs. [14, 15], in the continuum approximation, and has been tested against *ab initio* calculations at half-filling in Ref. [16].

In Fig. 2(a) we compare Eq. (9) (right) with experimental results from Ref. [3] already mentioned in Sec. 3.1. Clearly, the self-consistent V given by Eq. (9) for $\epsilon_r = 1$ is a much better approximation than the unscreened result of Eq. (7) (see inset). In Fig. 2(b) we show the gap Δ_g as a function of carrier density n for the exfoliated biased BLG device, with realistic values of chemical doping n_0 [5]. The gap is given by Eq. (4), with $t_{\perp} \simeq 0.22$ eV [5] and V obtained by solving self-consistently Eq. (9) (left) for $\epsilon_r = 1$. Note that for $E_{ext} = 0$ we always have $E_{int} = 0$ (the charge imbalance must be externally induced), and therefore we also have $V = 0$ and $\Delta_g = 0$. For this particular biased BLG device the present model predicts $E_{ext} = 0$ for $n = 2n_0$, which explains the asymmetry for Δ_g vs n shown in Fig. 2(b). Note also that this device effectively provides a tunable gap semiconductor, as implied by Fig. 2(b): different gap values are achieved by tuning the gate voltage V_g , which controls the carrier density n . Note that the maximum Δ_g occurs when V_g reaches its maximum, which occurs just before the breakdown of SiO_2 . The breakdown field for SiO_2 is $\gtrsim 1$ V/nm, meaning that V_g values as high as 300 V are possible for the exfoliated BLG device. As shown in Sec. 3.1, $V_g \simeq \pm 300$ V implies $n - n_0 \simeq \pm 22 \times 10^{12} \text{ cm}^{-2}$, and therefore Fig. 2(b) nearly spans the interval of possible densities. It is apparent, specially for $n_0 = 5.4 \times 10^{12} \text{ cm}^{-2}$, that when the maximum allowed densities are reached the gap seems to be approaching a saturation limit. This saturation is easily identified with the plateau shown in Fig. 1(d) for Δ_g vs V , occurring for $V \gtrsim t_{\perp}$. We may then conclude that this device enables the entire range of allowed gaps (up to t_{\perp}) to be accessed.

4. Edge states in bilayer graphene

The study of edge states in AB -stacked BLG given here is based on the ribbon geometry with zigzag edges shown in Fig. 3(a). Zigzag edges break translational invariance along their perpendicular direction, enabling us to write an effective one-dimensional Hamiltonian for a given momentum $ka \in [0, 2\pi[$ along the ribbon. The first nearest-neighbor tight-binding Hamiltonian [Eq. (1)] can then be written as

$$H_k = -t \sum_{i=1}^2 \sum_n a_{i;k,n}^\dagger (-e^{ika/2} D_k b_{i;k,n} + b_{i;k,n-1}) - t_\perp \sum_n a_{1;k,n}^\dagger b_{2;k,n} + \text{h.c.}, \quad (10)$$

where $a_{i;k,n}$ ($b_{i;k,n}$) is the annihilation operator at momentum k and position n across the ribbon in sublattice Ai (Bi), $i = 1, 2$ is the layer index and $D_k = -2 \cos(ka/2)$.

4.1. Semi-infinite bilayer graphene

Edge states in BLG are investigated by solving the Schrödinger equation, $H_k |\psi_k\rangle = E_k |\psi_k\rangle$. An analytic solution is possible for the semi-infinite BLG [17], the same being true for SLG [12]. The wavefunction $|\psi_k\rangle$ is written as a linear combination of the site amplitudes along the edge's perpendicular direction, $|\psi_k\rangle = \sum_n \sum_{i=1}^2 [\alpha_i(k, n) |a_i, k, n\rangle + \beta_i(k, n) |b_i, k, n\rangle]$, where we have introduced the one-particle states $|c_i, k, n\rangle = c_{i;k,n}^\dagger |0\rangle$, with $c_i = a_i, b_i$. Assuming all edge atoms belong to the A sublattice (without loss of generality), we require the boundary conditions $\alpha_i(k, n \rightarrow \infty) = \alpha_i(k, -1) = \beta_i(k, n \rightarrow \infty) = \beta_i(k, -1) = 0$, with $i = 1, 2$, accounting for the existence of the edge at $n = 0$. Within our model, the Fermi energy of BLG always occurs at zero energy. Therefore, we expect zero energy edge states to have interesting physical consequences, and we set $E_k = 0$. As a result, the two sublattices become completely decoupled, and only the sublattice to which edge atoms belong can support edge states. This means that we always have $\beta_1(k, n) = \beta_2(k, n) = 0$.

With H_k as in Eq. (10), it is easy to write $H_k |\psi_k\rangle = 0$ as a transfer matrix that relates $\alpha_i(k, n+1)$ with $\alpha_i(k, n)$, for $i = 1, 2$. Then, applying the abovementioned boundary conditions we find that bilayer graphene supports two types of zero energy edge states localized at zigzag edges for $2\pi/3 < ka < 4\pi/3$: one type restricted to a single layer and coined *monolayer family*, with amplitudes equivalent to edge states in SLG,

$$\alpha_1(k, n) = 0 \quad \text{and} \quad \alpha_2(k, n) = \alpha_2(k, 0) D_k^n e^{-i\frac{ka}{2}n}, \quad (11)$$

and a new type coined *bilayer family*, with finite amplitudes over the two layers,

$$\alpha_1(k, n) = \alpha_1(k, 0) D_k^n e^{-i\frac{ka}{2}n} \quad \text{and} \quad \alpha_2(k, n) = -\alpha_1(k, 0) D_k^{n-1} \frac{t_\perp}{t} e^{-i\frac{ka}{2}(n-1)} \left(n - \frac{D_k^2}{1 - D_k^2} \right), \quad (12)$$

where the normalization constants are given by $|\alpha_2(k, 0)|^2 = 1 - D_k^2$ and $|\alpha_1(k, 0)|^2 = (1 - D_k^2)^3 / [(1 - D_k^2)^2 + t_\perp^2/t^2]$. An example of the charge density associated with Eq. (12) is shown in Fig. 3(b) for $t_\perp = 0.2t$, where the $|\alpha_1(k, n)|^2$ dependence can also be seen as the solution given by Eq. (11) for $|\alpha_2(k, n)|^2$, apart from a normalization factor.

We note that the same value of λ , the penetration depth, is obtained from Eqs. (11) and (12): $\lambda = -1/\ln |D_k|$. Nevertheless, the solution given by Eq. (12) has a linear dependence in n which enhances its penetration into the bulk. We expect these states to contribute more to self doping than the usual SLG edge states [13], as the induced Hartree potential which limits the charge transfer between the bulk and the edge will be weaker.

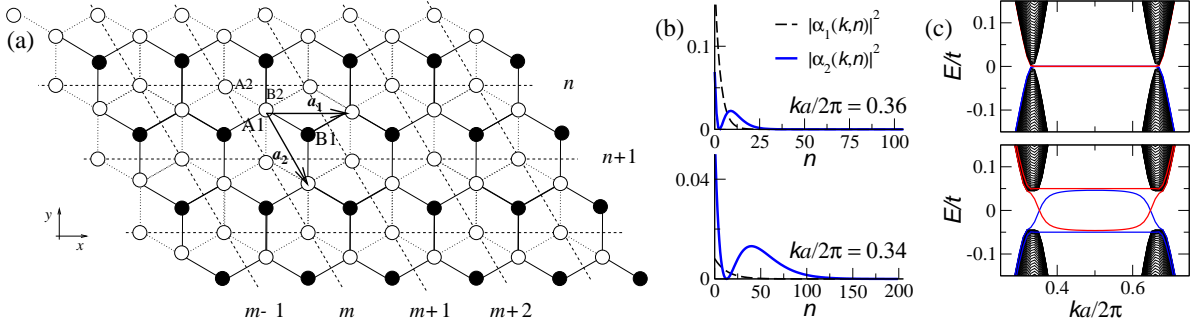


Figure 3. (a) Bilayer graphene ribbon with zigzag edges. (b) Charge density for bilayer edge states at $ka/2\pi = 0.36$ (top) and $ka/2\pi = 0.34$ (bottom). (c) Energy spectrum for a bilayer ribbon with zigzag edges, $N = 400$, $t_{\perp} = 0.2t$: $V = 0$ (top) and $V = t_{\perp}/2$ (bottom).

4.2. Bilayer zigzag ribbons

So far we studied localized states at the semi-infinite BLG. Experimentally, however, the relevant situation is a BLG ribbon. The band structure of a BLG ribbon with zigzag edges and N unit cells in the perpendicular direction is shown in the top panel of Fig. 3(c), obtained by numerically solving Eq. (10). There are four partly flat bands at $E = 0$ for k in the range $2\pi/3 \leq ka \leq 4\pi/3$, corresponding to four edge states, two per edge. Strictly speaking, the edge states given by Eqs. (11) and (12), and the other two localized at the opposite edge, are eigenstates of the semi-infinite system only. In the ribbon the overlapping of four edge states leads to a slight dispersion and non-degeneracy.

The fact that edge states do exist in BLG ribbons imply several interesting physical properties. First we note that edge states induce a strong peak in the density of states (DOS) at zero energy, due to the flatness of the energy bands. This DOS peak can be easily obtained as follows. Assuming we are sufficiently far from the Dirac points, and taking into account that $t_{\perp}/t \ll 1$ holds, we can write for the overlapping between monolayer and bilayer edge state families $|T_k^{\text{sl}}| \approx t|D_k|^N$, while the overlapping between two edge states of the bilayer family can be written as $|T_k^{\text{bl}}| \approx t_{\perp}N|D_k|^{N-1}$ (the overlapping between two edge states of the monolayer family being identically zero). The energy dispersion may then be approximated by $E_k \approx \pm|D_k|^N [(4t^2 + t_{\perp}^2 N^2/D_k^2)^{1/2} \pm t_{\perp}N/|D_k|]$, which, near $ka \sim \pi$ and assuming $N \gg 1$, can be further simplified as

$$E_k \sim \begin{cases} \pm t_{\perp}N|ka - \pi|^N \\ \pm t^2|ka - \pi|^N/(t_{\perp}N) \end{cases} . \quad (13)$$

Thus the DOS induced by edge states has the form $\rho(E) \sim E^{-1+\frac{1}{N}}/N$, which is also found in SLG. Therefore, as predicted for SLG [18], we expect a Curie-like temperature dependence for the Pauli paramagnetism in BLG due to edge states – twice as large due to the presence of twice as many edge states in BLG. Furthermore, edge magnetism (close to zero temperature) was found to be possible in BLG due to edge states [19], similarly to SLG [12].

Of particular importance is the effect of a perpendicular electric field applied to the zigzag bilayer ribbon. The semi-infinite biased system has only one edge state given by Eq. (11), as the edge state having finite amplitudes at both layers [Eq. (12)] is no longer an eigenstate. In the bottom panel of Fig. 3(c) we show the band structure of a BLG ribbon for $V = t_{\perp}/2$. Two partially flat bands for k in the range $2\pi/3 \leq ka \leq 4\pi/3$ are clearly seen at $E = \pm V/2$. These are bands of edge states localized at opposite ribbon sides, with finite amplitudes on a single layer [Eq. (11)]. Also evident is the presence of two dispersive bands crossing the gap, which are reminiscent of the bilayer family of edge states. This dispersive states appearing inside the gap

may contribute to the finite spectral weight recently observed using ARPES [3].

5. Conclusions

We have studied the electronic behavior of BLG using the minimal tight-binding model that describes the system. Particular focus has been given to the presence of an external electric field perpendicular to the BLG system – *biased bilayer* – which gives rise to a finite gap in the spectrum, whose size is completely controlled by the applied voltage. The effect of the perpendicular electric field has been included through a parallel plate capacitor model, with screening correction at the Hartree level. The biased BLG thus realizes the first tunable gap semiconductor – a proof of principle regarding real applications of BLG. We have also addressed the effect of zigzag edges in BLG. We have found that BLG, as its SLG counterpart and other graphene based materials [20], possesses zero energy surface states which can be divided into two families, giving rise to twice as many zero energy bands as in SLG. In the biased case half of the bands become dispersive inside the gap.

References

- [1] Novoselov K, Geim A, Morozov S, Jiang D, Zhang Y, Dubonos S, Grigorieva I and Firsov A 2004 *Science* **306** 666
- [2] Castro Neto A H, Guinea F, Peres N M R, Novoselov K S and Geim A K The electronic properties of graphene arXiv:0709.1163v1 [cond-mat.other]
- [3] Ohta T, Bostwick A, Seyller T, Horn K and Rotenberg E 2006 *Science* **313** 951
- [4] Oostinga J B, Heersche H B, Liu X, Morpurgo A F and Vandersypen L M K 2008 *Nat. Mater.* **7** 151 – 157
- [5] Castro E V, Novoselov K S, Morozov S V, Peres N M R, Lopes dos Santos J M B, Nilsson J, Guinea F, Geim A K and Castro Neto A H 2007 *Phys. Rev. Lett.* **99** 216802
- [6] Novoselov K S, McCann E, Morozov S V, Falko V I, Katsnelson M I, Zeitler U, Jiang D, Schedin F and Geim A K 2006 *Nat. Phys.* **2** 177–180
- [7] Castro E V, Peres N M R, Stauber T and Silva N A P 2008 *Phys. Rev. Lett.* **100** 186803
- [8] Nilsson J and Neto A H C 2007 *Phys. Rev. Lett.* **98** 126801
- [9] Castro E V, Peres N M R and Lopes dos Santos J M B 2007 *phys. stat. sol. (b)* **244** 2311
- [10] Chen Z, Lin Y M, Rooks M J and Avouris P 2007 *Physica E* **40** 228–232
- [11] Han M Y, Özyilmaz B, Zhang Y and Kim P 2007 *Phys. Rev. Lett.* **98** 206805
- [12] Fujita M, Wakabayashi K, Nakada K and Kusakabe K 1996 *J. Phys. Soc. Jpn.* **65** 1920–1923
- [13] Peres N M R, Guinea F and Castro Neto A H 2006 *Phys. Rev. B* **73** 125411
- [14] Nilsson J, Castro Neto A H, Guinea F and Peres N M R 2007 *Phys. Rev. B* **76** 165416
- [15] McCann E 2006 *Phys. Rev. B* **74** 161403
- [16] Min H, Sahu B, Banerjee S K and MacDonald A 2007 *Phys. Rev. B* **75** 155115
- [17] Castro E V, Peres N M R, Lopes dos Santos J M B, Castro Neto A H and Guinea F 2008 *Phys. Rev. Lett.* **100** 026802
- [18] Wakabayashi K, Fujita M, Ajiki H and Sigrist M 1999 *Phys. Rev. B* **59** 8271–8282
- [19] Castro E V, Peres N M R and Lopes dos Santos J M B Magnetic structure at zigzag edges of graphene bilayer ribbons arXiv:0801.2788v1 [cond-mat.mes-hall]
- [20] Castro E V, Peres N M R and dos Santos J M B L Localized states at zigzag edges of multilayer graphene and graphite steps arXiv:0805.2161v1 [cond-mat.mes-hall]